Petroleum Science 23 (2026) 582–595

Contents lists available at ScienceDirect

Petroleum Science

journal homepage: www.keaipublishing.com/en/journals/petroleum-science

Original Paper

Geochemical characteristics and sources of natural gas in the Upper Paleozoic limestone strata, Ordos Basin

Wen Zhang [a], Qian-Ping Wang [b], Wen-Hui Liu [a,*], Ping-Ping Shi [b], Hou-Yong Luo [c], Peng Liu [a,d], Xiao-Yan Chen [a,*], Qian Zhang [c], Xiao-Feng Wang [a], Dong-Dong Zhang [a], Yi-Ran Wang [a], Fu-Qi Li [e]

[a] State Key Laboratory of Continental Dynamics, Department of Geology, Northwest University, Xi'an, 710069, Shaanxi, China
[b] Exploration and Development Research Institute of PetroChina Changqing Oilfield Company, Xi'an, 710018, Shaanxi, China
[c] College of Chemistry and Chemical Engineering, Shaanxi Key Laboratory of Chemical Additives for Industry, Shaanxi University of Science and Technology, Xi'an, 710021, Shaanxi, China
[d] College of Safety Science and Engineering, Xi'an University of Science and Technology, Xi'an, 710054, Shaanxi, China
[e] Natural Gas Research Institute Branch, Shaanxi Yanchang Petroleum (Group) Company, Ltd., Xi'an, 710061, Shaanxi, China

ARTICLE INFO

Article history:
Received 19 December 2024
Received in revised form
22 July 2025
Accepted 12 October 2025
Available online 17 October 2025

Edited by Xi Zhang and Jie Hao

Keywords:
Taiyuan Formation
Natural gas
Position-specific carbon isotope
Geochemical characteristics
Ordos Basin

ABSTRACT

The discovery of high-yield industrial gas flows in the limestone layer of the Permian Taiyuan Formation in the Ordos Basin highlights promising prospects for natural gas exploration and has positioned this region as a key exploration area. However, research on the origin and distribution of natural gas in the Taiyuan Limestone Formation, especially its hydrocarbon generation potential and whether these organically enriched limestones can serve as effective source rocks, remains limited. In this study, we aimed to analyse the composition and carbon isotopes of the Upper Palaeozoic Taiyuan Limestone Formation natural gas, including propane-specific isotopes. The isotopic data were compared with coal-type gases from the corresponding strata and oil-type gases from the Lower Palaeozoic carbonate strata. Natural gas in the Upper Palaeozoic Taiyuan Limestone Formation was markedly distinct from the 'self-generated and self-accumulated' oil-type gas in the Lower Palaeozoic subsalt strata, indicating no obvious correlation between the two gases. The results did not support the notion that large-scale natural gas accumulations in the Lower Palaeozoic carbonate formations could be originated from Upper Palaeozoic limestone source rocks. The natural gas in the Upper Palaeozoic Taiyuan Limestone Formation was highly consistent with the typical coal-type gas from the Upper Paleozoic. The geochemical characteristics of the natural gas in the region were consistent with that of conventional natural gas, the position-specific isotopic composition of propane Δ_{C-T} values had a narrow, positive. This showed that the gas in the Taiyuan Limestone Formation was derived from type III kerogen, and propane mainly generated through the n-C_3H_7 free radical pathway. Geochemical analyses of the Taiyuan Limestone source rocks, such as the determination of total organic carbon, kerogen carbon isotopes, organic macerals. Combined with the geochemical analysis of natural gas, it revealed low abundance of organic matter but good kerogen types, predominantly type II–III, at a late to high-maturity evolution stage. Although the formation had certain hydrocarbon generation potential, it falls short of the hydrocarbon generation capacity of the Carboniferous–Permian coal measure source rocks. At present, there is no large–scale hydrocarbon generation, and it is not enough to provide hydrocarbon for the Lower Paleozoic.

1. Introduction

The Ordos Basin is a typical cratonic superimposed basin in the west of North China plate. It contains multiple hydrocarbon-bearing strata and is extremely rich in oil and gas resources, making it one of the largest oil and gas production bases in China (Fu et al., 2022;

* Corresponding author.
E-mail addresses: whliu@nwu.edu.cn (W.-H. Liu), chenxiaoyan180401@163.com (X.-Y. Chen).
Peer review under the responsibility of China University of Petroleum (Beijing).

https://doi.org/10.1016/j.petsci.2025.10.008

Liu et al., 2024). The Mesozoic Triassic system in the basin is primarily exploited for tight oil and shale oil; the Upper Paleozoic Permian and Carboniferous systems are mainly for tight gas and coalbed methane; the Lower Paleozoic is dominated by natural gas from the top weathering crust of the Ordovician Majiagou Formation (Kong et al., 2024; Li et al., 2018, 2023; Liu et al., 2022; Yang et al., 2015; Zhang et al., 2023). Owing to the dense lithology of the Permian Taiyuan Formation limestone, only a few wells, such as ZH2 and ZH3, produced industrial gas after acidification during early exploration. However, the productivity of these individual wells is low, and they are largely overlooked by production units (Liu et al., 2024). Recently, the China Petroleum Changqing Oilfield Company revitalized the research and exploration deployment of the Taiyuan Limestone Formation in order to expand exploration areas. Two wells, YT1H and ZT1H, were drilled as part of the risk exploration. The YT1H well test obtained a high-yield natural gas unimpeded flow rate of 54.86×10^4 m^3/d, and the ZT1H well test obtained a natural gas unobstructed flow rate of 12.50×10^4 m^3/d (Li et al., 2024; Xiao et al., 2024). It is announced that Taiyuan Limestone Formation has made major breakthrough in natural gas exploration, showing that Taiyuan Limestone Formation has good natural gas exploration potential as a new production layer.

Extensive geochemical studies of natural gas indicate, natural gas in the Upper Palaeozoic Carboniferous–Permian marine-terrigenous and continental clastic reservoirs typically exhibit 'self-generated and self-accumulated' or 'near-source accumulation' characteristics. It originates mainly from the region's widespread coal measure source rocks (Guo et al., 2022; Yang et al., 2014; Yao et al., 2018). However, owing to limited research on Taiyuan Formation carbonate source rocks and natural gas, whether Taiyuan Limestone Formation natural gas has similar reservoir forming characteristics with clastic reservoir natural gas needs to be further studied.

The sedimentary environment of the Taiyuan period in the basin is characterized by continuous transgression, with a sedimentary palaeotopography of 'high in the north and low in the south'. This led to the development of a mixed marine–continental interactive sedimentary system comprising carbonate rocks, coal seams, and terrigenous clastics described as 'sand in the north and limestone in the south'. To the south of Yulin is epeiric sea carbonate deposit, with the limestone thickness of 5–30 m, which thins progressively to the north (Yang et al., 2025; Zhang et al., 2024). Drilling and outcrops reveal that Taiyuan Limestone Formation is mainly dark grey micritic limestone and bioclast micritic limestone, containing a large number of broad-sea salt organism fossil and algae lattice dissolved pores, marine and marine-continental transitional facies biological mixed (Liu et al., 2023). Although these bioclastic-rich limestones likely generated hydrocarbons on a large scale during the long-buried evolution process, their effectiveness as consistent geochemical source rocks requires systematic evaluation.

Hence, in this study, we aimed to clarify the origin and source of natural gas in the Taiyuan Formation. Limestone samples and natural gas samples were systematically collected from the Taiyuan Formation in the central and eastern parts of the basin. The natural gas composition, hydrocarbon isotope distribution, and propane-specific positional isotopic data were analysed and compared with the Upper Palaeozoic Carboniferous-Permian typical coal-type and Lower Palaeozoic marine-origin natural gas data. A propane-specific positional isotope index was introduced to facilitate differentiation between coal-type and oil-type gases. The origin of the natural gas in the Taiyuan Formation was accurately clarified using comprehensive geochemical indices. Based on a comprehensive determination of the organic matter type, total organic carbon (TOC) content, and maturity of the Taiyuan Limestone Formation, the possibility of the Taiyuan Limestone Formation as a hydrocarbon source was assessed, and the contribution of the Taiyuan Limestone Formation to the present gas reservoir was preliminarily evaluated. Combined with the spatial distribution characteristics of the overlying and underlying coal measure source rocks of the Taiyuan Formation, the primary sources of natural gas in the Taiyuan Limestone Formation were analysed. Our findings provide an important reference value for revealing the formation mechanism of limestone natural gas in the Taiyuan Formation and its subsequent exploration and deployment.

2. Geological setting

The Ordos Basin is located in the western part of the North China Platform and is the second-largest petroleum-bearing basin in China (Fu et al., 2020). It is divided into six first–order tectonic units: Yimeng Uplift, Western Margin Thrust Belt, Tianhuan Depression, Yishan Slope, Jinxi Fault-fold Belt, and Weibei Uplift (Liu et al., 2009; Xiao et al., 2019; Xiong et al., 2020; Yang, 2022).

The Late Paleozoic marine–terrigenous sedimentary system was developed in the Ordos Basin. Marine and continental coal measures deposits were developed the Carboniferous (Xi et al., 2023). In the early Permian Taiyuan period, the scope of seawater intrusion in the eastern and western margins expanded further. The North China Sea and the Qilian Sea connected to form a unified coastal shallow sea deposit with coal measures as a typical feature, and lagoon and tidal flat deposits developed widely. The early Taiyuan Basin exhibits geomorphological feature of being higher in the north and lower in the south, with steeper northern and gentler southern slopes (Chen et al., 2010). Alluvial fans, deltas, and shallow-shelf marine sediments developed from north to south. A bioclastic beach developed in the Hengshan-Jingbian area, and a bioherm developed in the Zizhou–Qingjian area (Fig. 1 (a)) (Fu, 2023). Regional sea retreat occurred at the end of the Taiyuan period, seawater withdrew from the Ordos area during the Early Permian Shanxi to Late Permian Shiqianfeng periods, and the sedimentary pattern changed from east–west differentiation to north–south differentiation. The salinity of the water changed from brackish to fresh water, and a fluvial–delta–lacustrine sedimentary assemblage developed (Mao, 2020).

The paleoclimate of the Taiyuan period is warm and humid, and the sedimentary water body is marked by brackish water–fresh water, which is an important coal-forming period (Ma et al., 1999). Vertically, the Taiyuan Formation developed two third-order cycles from transgression to regression, among which the fourth-order cycle has a sedimentary filling mode of lithology from limestone to coal rock, 'north sand and south limestone, overlying mudstone–coal' on the plane. During the Shanxi period, the sedimentary environment changed from marine to continental facies, and the climate changed from humid to arid, forming a multi-period superimposed, large area zonal distribution of river–delta facies sand bodies (Mao, 2020). A mixed formation of carbonate rock, coal rock, and terrigenous clastic rock formed during the Lower Permian Taiyuan Formation. The thickness of the formation is generally 15–55 m (Chen and Liu, 1997; Fu et al., 2003; Xi et al., 2023). The Taiyuan Limestone Formation reservoirs include bioclastic limestone, micritic limestone, and dolomite interlayers (Fig. 1(b)) (Fu, 2023; Wang et al., 2024).

3. Samples and experiments

3.1. Samples

We performed a gas source correlation analysis for natural gas in the Taiyuan Limestone Formation reservoirs in the Ordos Basin.

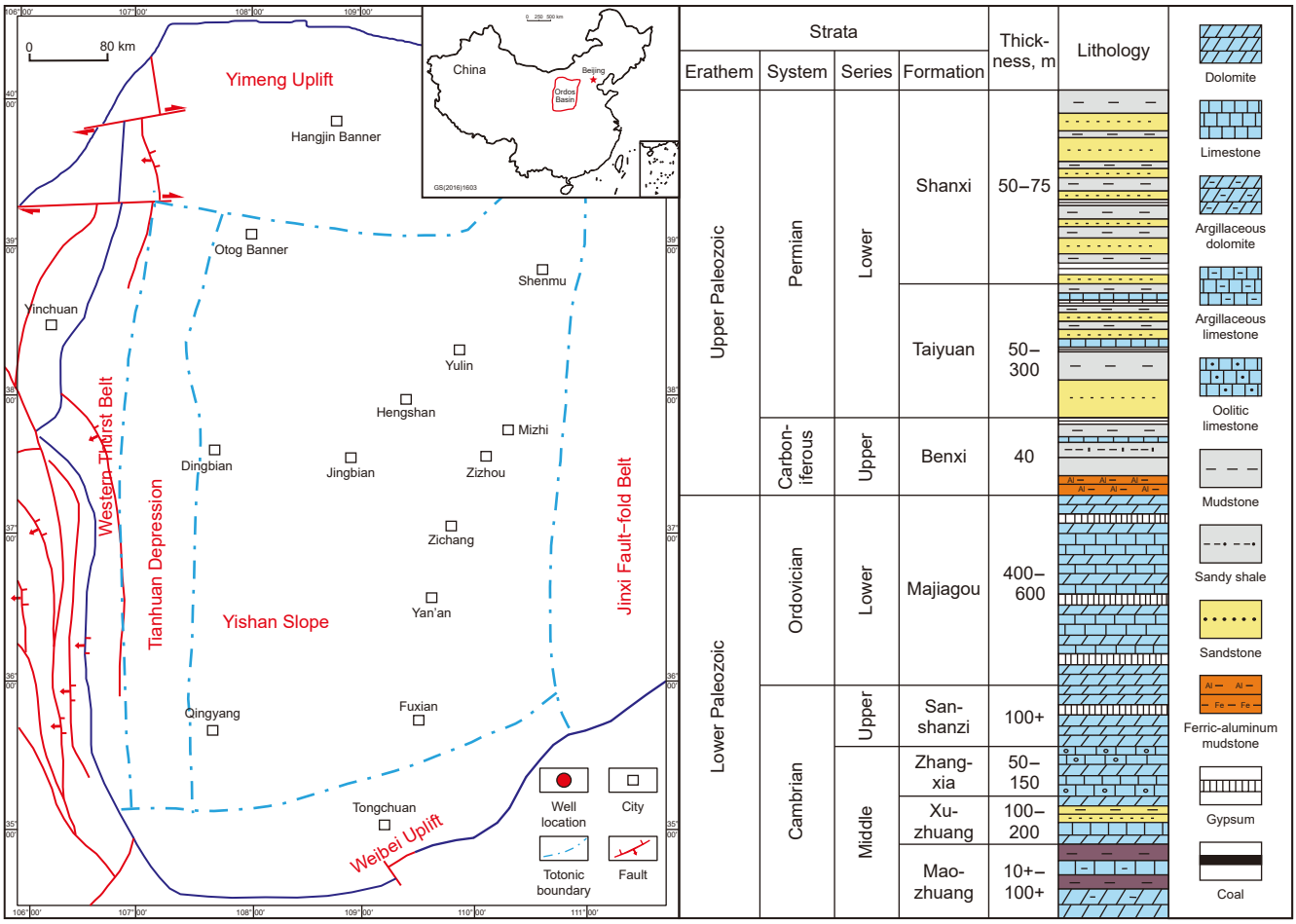

Fig. 1. Comprehensive histogram of tectonic unit division and Paleozoic lithology in the Ordos Basin.

Plenty of literature research, data collection, and analysis tests were carried out in the central and eastern part of the Ordos Basin. 32 natural gas samples such as J102 well, J9 well, and YT1H well were collected and analysed. Simultaneously, a number of geochemical analyses of Upper Paleozoic natural gas, including 89 in Shanxi Formation, 42 in Taiyuan Formation and 14 in Shihezi Formation, were collected. 14 samples of the Taiyuan Limestone Formation (Zhaoxian section in Lin County, Shanxi Province) were collected, and their geochemical characteristics were analysed.

3.2. Geochemical and stable isotope analysis

3.2.1. Natural gas components and isotope analysis

The experimental analysis was performed at the Stable Isotope Geochemistry Laboratory, State Key Laboratory of Continental Dynamics, Northwest University, Xi'an, China. The components of the natural gas samples were determined using an Agilent Technologies 7890B Gas Chromatograph (GC) (Yu et al., 2015). The analysis program was run as follows. The initial temperature of the GC oven was set at 80 °C; it was first heated to 100 °C at a rate of 5 °C/min, maintained for 2 min, then heated to 290 °C at a rate of 10 °C/min, and maintained for 3 min. The measured components of natural gas are expressed as percentages, %.

The carbon isotope composition of natural gas was determined using a Thermo Scientific Delta XP Plus IRMS combined with an HP5890 II gas chromatograph equipped with a capillary column (PLOT-Q, 30 m × 0.32 mm). The test procedure was as follows. The GC oven was initially heated to 80 °C at a rate of 8 °C/min; thereafter, it was heated to 260 °C at a rate of 10 °C/min and maintained for 10 min until the measurement was completed. The $\delta^{13}C$ values of gases are reported in per mil (hundred meters, ‰) relative to the V-PDB standard, and the δD values are reported in per mil (hundred meters, ‰) relative to the V-SMOW standard. The measurement accuracies of both the $\delta^{13}C$ and δD values were within ±0.3‰.

3.2.2. Position-specific isotope composition

The position-specific carbon isotope composition of propane in the gas samples was measured using GC-pyrolysis-GC-C-IRMS (Gilbert et al., 2016). The tests included separation and pyrolysis. High-purity helium gas was used as the carrier gas, and deactivated fused silica capillary columns (0.25 mm inner diameter) were used to connect the devices. Natural gas samples were first separated by the first gas chromatographic column (HP-PLOT-Q, 30 m × 0.32 mm inner diameter). The initial temperature of the GC oven was set at 50 °C for 3 min, the temperature was then raised to 200 °C at a rate of 10 °C/min and maintained for 8 min. Once the separated product entered the ceramic tube reactor, and the pyrolysis process began in a 790 °C pyrolysis furnace. After that, it was separated again using a second gas chromatography, with the

oven maintained at 30 °C. The separated fragments entered GC-Isolink II and were burned to CO_2 at 1000 °C. The $\delta^{13}C$ values were measured using a Thermal Scientific MAT 253 Plus IRMS.

Gilbert et al. (2016) found that methane was formed from the methyl group of propane and ethane was formed by the splicing of two methyl groups of propane formed during pyrolysis. In this study, the position-specific isotope distribution of propane was calculated using Eqs. (1)–(3).

$$\Delta_{C-T} = \delta^{13}C_{central} - \delta^{13}C_{terminal} \quad (1)$$

$$\delta^{13}C_{terminal} = \left(\delta^{13}C_{methane} \times S_{methane} + \delta^{13}C_{ethane} \times S_{ethane}\right) / \left(S_{methane} + S_{ethane}\right) \quad (2)$$

$$\delta^{13}C_{terminal} + \delta^{13}C_{central} = 2 \times \delta^{13}C_{ethylene} \quad (3)$$

In the equations, $S_{methane}$ and S_{ethane} are the areas of the CO_2 peak in the IRMS spectra of methane and ethane, respectively. The carbon isotopic composition at specific propane position was corrected as described by Liu et al. (2023). For samples with a low propane content, the C_{2+} hydrocarbon components were analysed and determined after enrichment. The measurement accuracy of propane position-specific carbon isotope composition in this study is within ±1.0‰.

3.2.3. Hydrocarbon source rock

The experimental analysis was performed at the Stable Isotope Geochemistry Laboratory, State Key Laboratory of Continental Dynamics, Northwest University. TOC analysis was performed using a LECO CS744 carbon-sulfur analyser. The TOC testing process included the following steps. First, the sample was crushed and ground to a mesh size of < 80. The sample powder was then placed in a permeable crucible and weighed accurately. Finally, hydrochloric acid (HCl) was added and dissolved in a water bath at 80 °C for 12 h and heated for 3 h to remove carbonate minerals (Li Y.N. et al., 2021; Wang et al., 2025).

Rock Pyrolysis was performed using a Rock-Eval 6 Pyrolysis Analyzer. In the pyrolysis experiment, the source rock needs to be maintained at a constant temperature of 300 °C for 3 min to estimate S_1. Subsequently, the temperature is elevated from 300 to 650 °C at a rate of 25 °C/min for the temperature-rise analysis to estimate S_2 (Han et al., 2018a).

The EA IsoLink-IRMS system was used to measure the kerogen organic carbon isotope composition of source rocks. The sample pretreatment method includes, the sample powder less than 80 mesh was placed in the permeable crucible for weighing, and dilute hydrochloric acid was continuously added to the crucible until no gas was produced. The sample was then washed in an 80 °C water bath with distilled water for neutralisation and placed in a 50 °C oven for drying. The dried sample was placed in a tin cup and analysed using a Flash 2000 HT elemental analyser (Zhang et al., 2024).

The vitrinite reflectance (R_o) was determined using a Leica DM4500P polarising microscope with a 50 × objective lens, yielding a random reflectance value under oil-immersion conditions.

4. Results

4.1. Geochemical characteristics of natural gas

The composition characteristics of natural gas components and the carbon and hydrogen isotope composition are listed in Table 1. The natural gas composition in the Permian Taiyuan limestone reservoirs was dominated by hydrocarbons, with methane being the predominant gaseous hydrocarbon component with an average of 88.48%. The dryness coefficient ($C_1/\Sigma C_{1-5}$) of the gas ranged from 0.960 to 0.991, with a mean value of 0.974, exhibiting characteristics of 'dry gas' and being drier compared to the other

Table 1
The geochemical characteristics of Upper Paleozoic natural gas in the Ordos Basin.

Strata		Taiyuan Limestone Formation	Taiyuan Formation limestone development region	Coal measure strata of Shihezi Formation	Coal measure strata of Shanxi Formation	Data source
Hydrocarbon components, %	CH_4	72.65–94.29 88.48(11)	80.08–98.23 91.30(22)	70.68–95.18 90.10(14)	81.07–95.65 92.76(87)	This study; Dai et al. (2005, 2014); Hu et al. (2007); Han et al. (2022); Huang et al. (2015); Li et al. (2014); Li et al. (2023); Liu et al. (2015); Li et al. (2021); Wu et al. (2019); Yang et al. (2015); Zhang et al. (2023); Zhao et al. (2014)
	C_2H_6	0.75–3.13 1.87(11)	1.00–7.15 4.03(22)	2.83–7.42 4.50(14)	2.01–10.57 4.00(87)	
	C_3H_8	0.06–0.53 0.27(11)	0.14–2.06 0.96(22)	0.19–2.48 0.80(14)	0.13–3.68 0.80(87)	
	iC_4H_{10}	0.01–0.20 0.10(11)	0.01–0.28 0.14(20)	0.04–0.38 0.14(11)	0.01–0.59 0.14(73)	
	nC_4H_{10}	0.01–0.11 0.05(11)	0.01–0.43 0.16(20)	0.04–0.51 0.18(14)	0.02–0.92 0.18(87)	
	C_1/C_{1-5}	0.960–0.991 0.974(11)	0.896–0.988 0.945(22)	0.883–0.966 0.941(14)	0.831–0.970 0.947(87)	
Non-hydrocarbon components, %	CO_2	1.47–7.21 3.55(9)	0.36–2.91 1.49(25)	0.10–1.22 0.47(10)	0.02–2.72 1.23(61)	
	N_2	0.15–14.54 4.91(10)	0.21–22.23 4.31(21)	0.04–19.82 3.75(11)	0.03–3.42 0.77(56)	
$\delta^{13}C$, ‰	CH_4	−33.4– − 31.7 −32.7(10)	−40.9– − 31.6 −36.0(33)	−38.3– − 30.9 −34.1(13)	−38.3– − 30.2 −32.9(89)	
	C_2H_6	−24.0– − 21.5 −22.3(10)	−32.2– − 22.0 −25.0(33)	−26.3– − 22.7 −24.6(13)	−27.0– − 22.7 −25.2(89)	
	C_3H_8	−23.7– − 19.7 −21.2(10)	−27.6– − 19.0 −23.3(31)	−25.2– − 22.3 −23.6(11)	−26.5– − 20.8 −23.4(89)	
δD, ‰		−190– − 170 −179(8)	−205– − 195 −201(6)	−183– − 182 −182(3)	−214– − 175 −186(41)	

* Minimum value–maximum value / Average value (The number of samples)

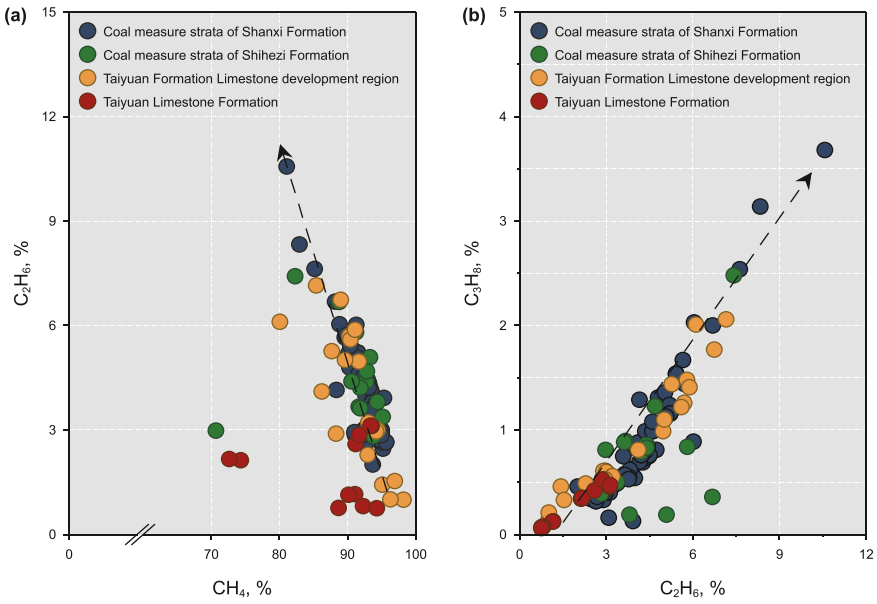

Fig. 2. Characteristics of natural gas components in different strata of the Upper Paleozoic in the Ordos Basin. **(a)** Scatter plot of CH_4–C_2H_6 in natural gas. **(b)** Scatter plot of C_2H_6–C_3H_8 in natural gas.

two groups of natural gas. The non-hydrocarbon components consisted mainly of CO_2 and N_2, with an average N_2 content of 4.91% and a generally low CO_2 content, averaging 3.55%. Overall, there was a strong negative correlation between methane and ethane contents, indicating that the methane content decreased as the ethane content increased (Fig. 2(a)). Individual samples had methane content as low as 72.65%, possibly because of the impact of reservoir modification during the production process.

Natural gas from the other Paleozoic strata consisted primarily of hydrocarbons. The methane content of the natural gas in Taiyuan Limestone Formation development region ranged from 80.08% to 98.23%, with an average of 91.30%, whereas the ethane content fell between 1.00% and 7.15%, with an average of 4.03%. The drying coefficient ranged from 0.896 to 0.988, with an average of 0.945. The average CO_2 content of the non-hydrocarbon components was 1.49%, the average N_2 content was 4.31%, H_2S was absent. The methane content of the natural gas in the Shanxi Formation and Shihezi Formation coal measure strata ranged from 81.07% to 95.65% and from 70.68% to 95.18%, respectively, with average values of 92.76% and 90.10%. The propane content ranged from 2.01% to 10.57% and 2.83%–7.42% respectively (Fig. 2(b)). The dryness coefficient of natural gas in Shanxi Formation ranged from 0.831 to 0.970 (with an average of 0.947) and that of natural gas in Shihezi Formation ranged from 0.883 to 0.966 (with an average of 0.941). Overall, the methane, ethane and propane contents of the limestone natural gas in the Taiyuan Formation had a narrow distribution range and were less than those of the coal-type natural gas in the Shanxi Formation

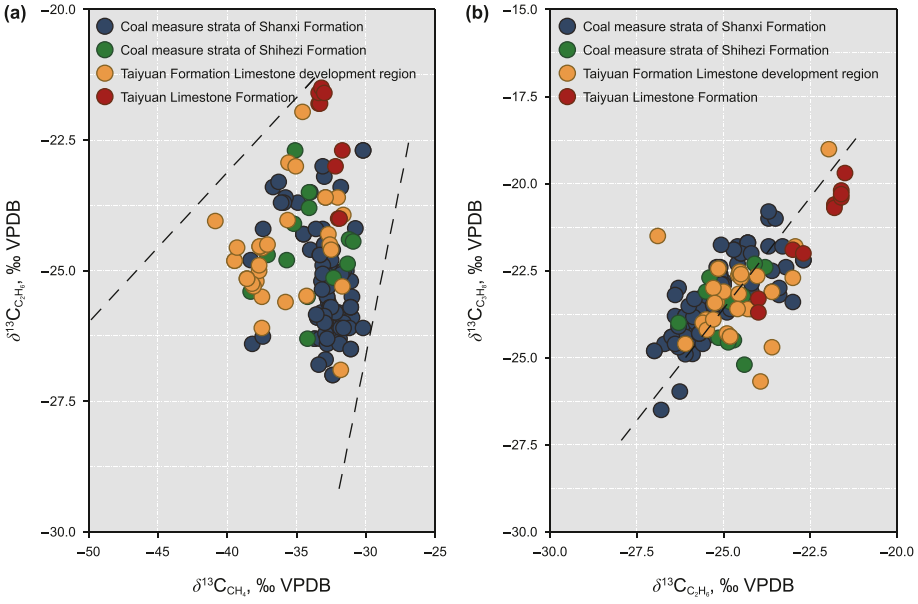

Fig. 3. Isotopic characteristics of natural gas in different strata of the Upper Paleozoic in the Ordos Basin. **(a)** Scatter plot of $\delta^{13}C_{CH_4}$–$\delta^{13}C_{C_2}H_6$ in natural gas. **(b)** Scatter plot of $\delta^{13}C_{C_2}H_6$–$\delta^{13}C_{C_3H_8}$ in natural gas.

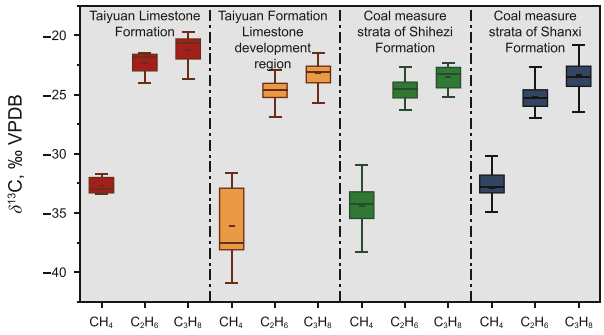

Fig. 4. Histogram of hydrocarbon composition distribution in the Upper Paleozoic natural gas in the Ordos Basin.

and Shihezi Formation; however, the non-hydrocarbon (CO_2, N_2) contents were higher than those of the coal-type natural gas in the Shanxi Formation and Shihezi Formation, and the difference was very obvious. If natural gas originated from the same set of hydrocarbon source rocks, the component contents should be relatively similar. It implies that the limestone natural gas in the Taiyuan Formation is different from the natural gas genesis of the coal measure source rock.

The $\delta^{13}C_1$ values of natural gas in Taiyuan Limestone Formation were distributed between −33.4‰ and −31.7‰ (with an average of −32.7‰); $\delta^{13}C_2$ ranged from −24.0‰ to −21.5‰ (with an average of −22.3‰), and $\delta^{13}C_3$ values ranged between −23.7‰ and −19.7‰ (the average of −21.2‰) (Fig. 3). The $\delta^{13}C_1$ values in Taiyuan Limestone Formation development region were distributed between −40.9‰ and −31.6‰ (the average value was −36.0‰), $\delta^{13}C_2$ varied between −32.2‰ and −22.0‰ (the average value was −25.0‰), and $\delta^{13}C_3$ values were distributed between −27.6‰ and −19.0‰ (the average value was −23.3‰). The $\delta^{13}C_1$ values of natural gas in the coal measure strata of Shihezi Formation were distributed between −38.3‰ and −30.9‰ (the average value was −34.1‰), $\delta^{13}C_2$ varied between −26.3‰ and −22.7‰ (the average value was −24.6‰), and $\delta^{13}C_3$ varied between −25.2‰ and −22.3‰ (the average value was −23.6‰). The $\delta^{13}C_1$ values of natural gas in the coal measure strata of Shanxi Formation were distributed between −38.3‰ and −30.2‰ (the average value was −32.9‰), $\delta^{13}C_2$ varied between −27.0‰ and −22.7‰ (the average value was −25.2‰), and $\delta^{13}C_3$ varied between −26.5‰ and −20.8‰ (the average value was −23.4‰) (Fig. 3).

The limestone gas of the Taiyuan Formation were more concentrated in terms of the carbon isotopes of CH_4, C_2H_6, and C_3H_8 than the natural gas in the Upper Palaeozoic coal-bearing strata, and the stable carbon isotope sequence showed positive sequence characteristics. With respect to the overall carbon isotope distribution range of alkane gases, the maximum, minimum, and average carbon isotopic compositions of methane and its homologs gradually increased with the increase in the number of carbon atoms in the molecule (Fig. 4).

4.2. Position–specific carbon isotope composition of propane

The specific positional carbon isotope composition of natural gas is listed in Table 2. The Δ_{C-T} value of natural gas in the Taiyuan Limestone Formation ranged from 2.6‰ to 5.9‰, with an average of 4.4‰; the Δ_{C-T} value of natural gas in the Upper Paleozoic coal measure strata were more widely distributed, ranging from 0.8‰ to 4.8‰, with an average of 2.6‰. The relationship between $\delta^{13}C_3$ value and Δ_{C-T} value of natural gas from different layers is shown in Fig. 5. A positive correlation was observed between $\delta^{13}C_3$ and Δ_{C-T} values.

The terminal carbon position of propane is less influenced by microbial oxidation and is more closely related to the maturity and precursor associations. Therefore, the $\delta^{13}C_{terminal}$ value has great potential in informing the origin and maturity levels of natural gas. Fig. 6 illustrates the relationship between the $\delta^{13}C_{terminal}$ value and the $\delta^{13}C_1$, $\delta^{13}C_2$, and $\delta^{13}C_3$ values. The $\delta^{13}C_{terminal}$ value exhibited a narrow distribution range, and for most natural gas samples, the carbon isotope compositions of methane, ethane, and propane were positively correlated with the $\delta^{13}C_{terminal}$ values. Methane and ethane were associated with the terminal methyl group of propane, and the related pyrolysis reaction kinetics resembled the pyrolysis reaction kinetics published by Gilbert et al. (2016).

Table 2
Position-specific isotope compositions of Upper Paleozoic natural gas in the Ordos Basin.

Strata	Sample	Position-specific carbon isotope composition		
		Δ_{C-T}, ‰	$\delta^{13}C_{central}$, ‰	$\delta^{13}C_{terminal}$, ‰
Taiyuan Limestone Formation	J9-20TH1-1	4.9	−20.0	−24.9
	J72-22TH4-1	3.0	−18.3	−21.4
	J72-22TH4-2	2.6	−18.5	−21.1
	J102-63H2-1	5.4	−18.2	−23.7
	J102-63H2-3	5.9	−18.0	−23.9
Coal measure strata	Su41-8	1.6	−24.7	−25.6
	Su16	1.8	−22.9	−23.7
	Su38-14	0.9	−23.9	−25.3
	Su13-16	0.9	−22.8	−24.2
	Su25	1.4	−22.7	−24.5
	Su40-16	1.5	−23.5	−25.1
	D1-4-59-1	3.0	−21.8	−24.8
	D1-4-59-2	3.5	−21.1	−24.6
	D1-4-121	3.6	−20.5	−24.2
	JIN11	2.3	−22.8	−25.2
	JIN18	2.7	−21.4	−24.1
	JIN26	2.1	−23.1	−25.2
	DPH-30	1.5	−24.9	−26.5
	D1-4-72	4.1	−20.1	−24.2
	D1-4-122	4.1	−20.5	−24.7
	DPT-17	4.8	−19.4	−24.2
	D1-4-84	3.2	−19.6	−22.8
	D1-4-100	3.7	−20.3	−24.1

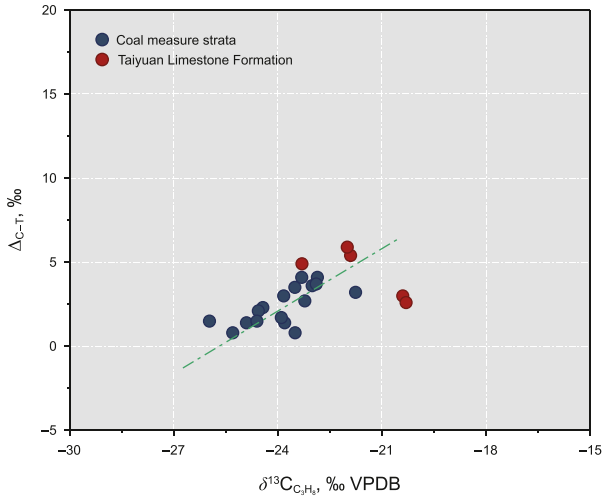

Fig. 5. Δ_{C-T}–$\delta^{13}C_{C_3H_8}$ for the propane from the Upper Paleozoic natural gas on the Ordos Basin.

4.3. Geochemical characteristics of hydrocarbon source rock

The analysis and testing data of the Zhaoxian section Taiyuan Limestone Formation outcrop samples are presented in Tables 3 and 4, respectively. The $\delta^{13}C$ values ranged from −27.8‰ to −24.1‰, with an average of −25.7‰; TOC ranged from 0.03% to 6.11%, with an average of 0.73%.

5. Discussion

5.1. Differences in geochemical characteristics of natural gas

The carbon isotope composition of organic natural gas is related to the type of organic parent material in the source rock and influenced by the degree of organic matter thermal evolution and the migration, accumulation, and reservoir formation methods of natural gas. Methane carbon isotopes are significantly influenced by the degree of thermal evolution of the hydrocarbon source rocks, whereas ethane carbon isotopes exhibit strong inheritance from the original organic matter. They are far less affected by the degree of thermal evolution of the source rocks than methane carbon isotopes, can reflect the characteristics of their parent materials to some extent, and are widely used in the identification of coal-type gas and oil-type gases. Dai (1992) pointed out that $\delta^{13}C_2 > -28‰$ indicates coal-type gas, whereas $\delta^{13}C_2 < -28‰$ indicates oil-type gas. They prepared $\delta^{13}C_1 - \delta^{13}C_2 - \delta^{13}C_3$ alkane gas type identification plate (Fig. 7), based on which, the natural gas in Taiyuan Limestone Formation, Taiyuan Limestone Formation development region, Shanxi Formation and Shihezi Formation were recognised as coal-type gas. This funding is consistent with the fact that the natural gas in Shanxi Formation and Shihezi Formation originate from the coal measure source rocks of the Upper Palaeozoic Carboniferous–Permian strata.

According to the natural gas genesis identification chart proposed by Milkov (2021), the natural gas in the Taiyuan Limestone Formation, Shanxi Formation and Shihezi Formation fall in the typical coal-type gas area, and the natural gas in the individual Taiyuan Limestone Formation development area falls in the oil-type gas area (Fig. 8), which may be related to the marine source. Compared to the 'self-generated and self-accumulated' natural gas in the Ordovician Majiagou Formation sub-salt strata ($Ma5_6$ Sub-member–Ma4 Member) in Ordos Basin. Taking the natural gas of the Ordovician middle assemblage ($Ma5_{5-10}$ submumber) in well SH97 and well SH99 in the Shenmu area as examples, the dry coefficient is 0.85, and the carbon isotope composition of alkane gases was significantly lighter than that in the Upper Paleozoic coal-type gas in this region. Among them, the $\delta^{13}C_1$ value was −44.7‰, the $\delta^{13}C_2$ value was −31.2‰, and the $\delta^{13}C_3$ value was −28.7‰, exhibiting typical oil-type gas characteristics (Kong et al., 2024). Although some samples exhibited the characteristics of coal-type gas, they did not represent true coal-type gas. Instead, intense thermal sulfate reduction (TSR) consumed ethane and propane, leading to the enrichment of heavy carbon isotopes and creating an illusion of coal-type gas. Fundamentally, it remains an oil-type gas (Liu et al., 2022). The gas in the Taiyuan Limestone Formation, although also stored in carbonate rock formations, does not exhibit characteristics typical of oil-type gas. Vertically, there was a thick layer of gypsum-salt rock between them, which exhibited excellent sealing properties, implying no genetic

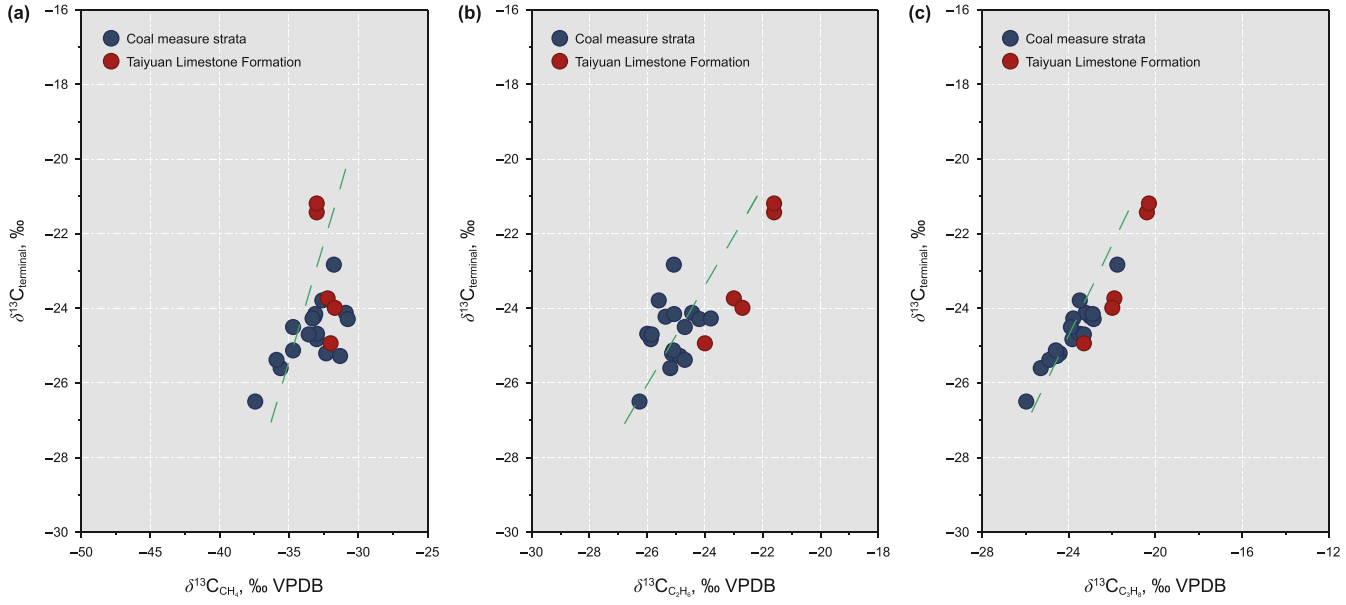

Fig. 6. The propane from the Upper Paleozoic natural gas in the Ordos Basin. **(a)** $\delta^{13}C_{terminal}$–$\delta^{13}C_{CH_4}$. **(b)** $\delta^{13}C_{terminal}$–$\delta^{13}C_{C_2H_6}$. **(c)** $\delta^{13}C_{terminal}$–$\delta^{13}C_{C_3H_8}$.

Table 3
Carbon isotope value of kerogen and TOC of the permian Taiyuan limestone formation in the Ordos Basin.

Sample number	Strata	Carbon isotope value, ‰	TOC, %
ZX-6-1	Taiyuan Formation	−27.8	0.19
ZX-6-2	Taiyuan Formation	−27.6	0.16
ZX-7	Taiyuan Formation	−24.1	0.40
ZX-8	Taiyuan Formation	−25.0	0.33
ZX-9	Taiyuan Formation	−24.3	0.39
ZX-10	Taiyuan Formation	−26.4	0.38
ZX-12-1	Taiyuan Formation	−26.1	0.11
ZX-12-2	Taiyuan Formation	−24.2	1.07
ZX-13	Taiyuan Formation	−26.2	0.17
ZX-14	Taiyuan Formation	−24.7	0.20
ZX-15-1	Taiyuan Formation	−24.8	0.41
ZX-16	Taiyuan Formation	−25.9	0.13

correlation with the self-generated and self-accumulated oil-type gas in the Lower Paleozoic sub-salt strata.

During hydrocarbon generation evolution of sedimentary organic matter, kinetic fractionation and inheritance effects between the components of natural gas and carbon isotopes of the parent materials. ^{12}C is more easily enriched in hydrocarbons with lower number of carbon atoms, whereas ^{13}C is more enriched in hydrocarbons with high carbon number. Therefore, the carbon isotopic compositions of methane and its homologs in primary organic alkane gases without secondary action tend to have a normal carbon sequence of $\delta^{13}C_1 < \delta^{13}C_2 < \delta^{13}C_3$ (Dai et al., 2008; Ni et al., 2024). However, under actual geological conditions, carbon isotope sequence inversion of alkane gases often occurs. This may be attributed to the mixing of organic and inorganic natural gas, mixing of oil-type gas and coal-type gas, mixing of homologous gases from different periods, mixing of different source gases of the same type, or oxidation of natural gas by bacteria (Dai et al., 2014; Liu et al., 2019). The reversal of carbon isotope sequence may be caused by a single factor or a combination of multiple factors. The natural gas in the Shanxi Formation and Shihezi Formation showed a positive carbon sequence, whereas the natural gas in the Taiyuan Limestone Formation and Taiyuan Limestone Formation development region had a positive carbon sequence. However, there was a 'L'-shaped normal carbon sequence lifted upward owing to the heavy composition of $\delta^{13}C_2$, which may be affected by the humic coal measure source rocks in adjacent layers (Fig. 9).

The hydrogen isotope composition of natural gas is influenced by the type of organic matter in source rocks, thermal maturity, and water medium environmental conditions, which are often used to identify natural gas origins (Liu et al., 2008). In freshwater environments, natural gas derived from source rocks has lighter hydrogen isotopic compositions. Conversely, the natural gas formed in saline environments has a heavier hydrogen isotope composition. Moreover, the carbon and hydrogen isotopes of natural gas methane are positively correlated with thermal maturity. Typical marine sapropelic natural gas has a heavier

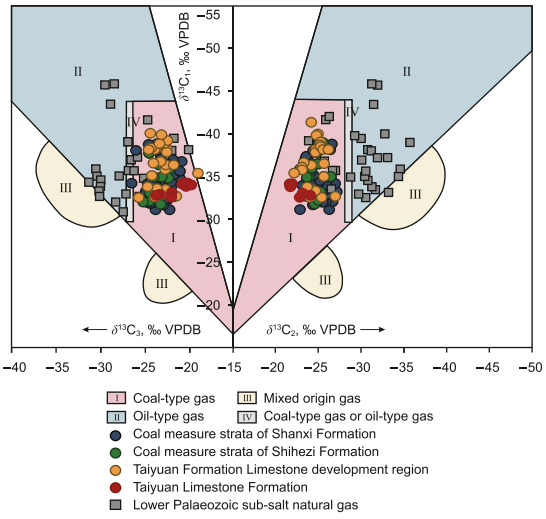

Fig. 7. $\delta^{13}C_{CH_4}$–$\delta^{13}C_{C_2H_6}$–$\delta^{13}C_{C_3H_8}$ natural gas type identification plate (modified from Dai, 1992, 2011).

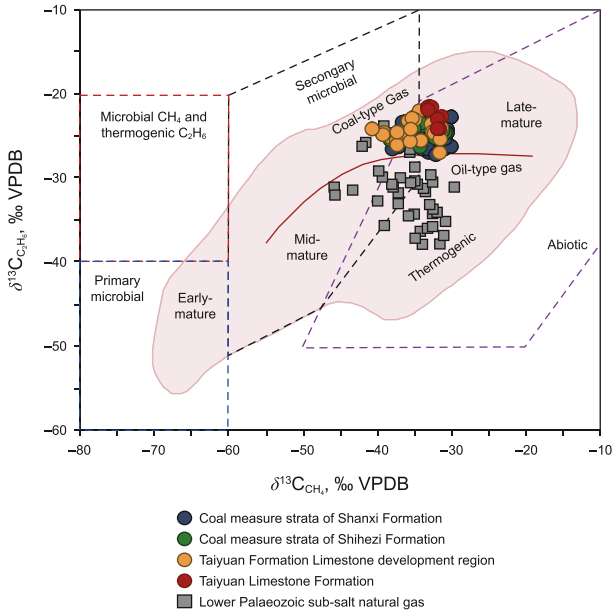

Fig. 8. $\delta^{13}C_{CH_4}$–$\delta^{13}C_{C_2H_6}$ natural gas type identification plate (modified from Milkov, 2021).

hydrogen isotope composition than typical coal-type gas, generally greater than −180‰. The hydrogen isotope composition of methane in typical coal-type gas only becomes greater than −180‰ at a very high thermal evolution degree (Wang et al., 2015).

Table 4
The geochemical characteristics of Upper Paleozoic in the Ordos Basin.

Region/strata	TOC, %	S_1+S_2, mg/g	I_H, mg/g	$\delta^{13}C$, ‰	R_o, ‰	T_{max}, °C
Taiyuan limestone formation	0.03–6.11 0.73(128)	0.01–2.53 0.33(117)	2–96 30(43)	−27.8– − 24.1 −25.6(48)	0.6–1.4 1.1(11)	301–608 509(44)
Coal	43.64–85.22 65.15(48)	1.74–310.36 94.08(48)	–	–	0.7–2.0 1.1(37)	447–591 483(44)
Mudstone	0.14–5.86 2.15(106)	0.09–69.60 2.38(106)	–	−27.6– − 22.9 −23.7(13)	0.7–1.6 1.0(66)	312–576 470(132)
Data source	This study; Fu (2023); Han et al. (2022); Li (2018); Luo et al., (2024); Zhang (2012); Zhao (2013)					

* Minimum value–maximum value / Average value (The number of samples).

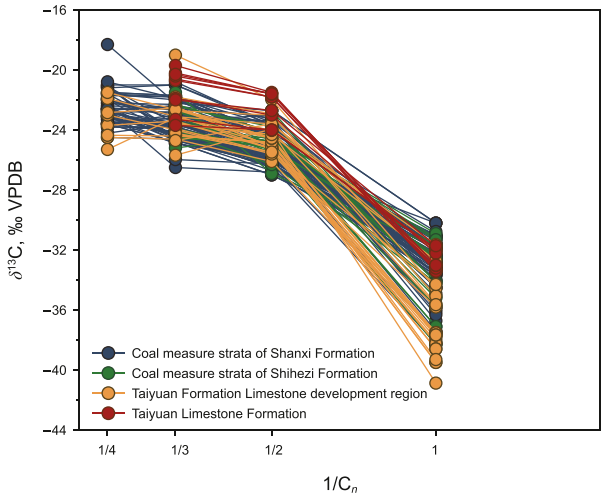

Fig. 9. The carbon isotope sequence diagram of natural gas in the Odors Basin.

In the methane carbon-hydrogen isotope plate of natural gas (Wang et al., 2015), the Taiyuan Limestone Formation gas consistently exhibited characteristics typical of coal measure source rocks. The δD composition of the Taiyuan Limestone Formation gas was slightly enriched, with some values exceeding −180‰, reflecting its high thermal maturity (Fig. 10(a)). Additionally, the combination of methane hydrogen and ethane carbon isotopes effectively distinguished between typical marine sapropelic natural gas and humic natural gas. As shown in Fig. 10(b), the natural gas in Taiyuan Limestone Formation remained primarily coal-type gas, which is consistent with the characteristics of typical coal-type gas from the Shanxi Formation and Shihezi Formation.

5.2. Identify the structural composition of the precursor by using the position isotope of propane

Specific position isotope analysis is primarily used to determine the isotopic composition of molecules, providing a deeper understanding of precursor reaction paths and chemical structures (Jin and Rolle, 2016; Julien et al., 2016). Propane is the smallest organic molecule with different carbon atoms, and different cracking pathways (at the terminal or central carbon positions) demonstrate different isotope fractionation. n-C_3H_7 and i-C_3H_7 capture hydrogen atoms to form the propane, where the free radicals are formed by the elementary cracking of precursors at different carbon positions. According to previous calculations, the $\delta^{13}C$ value of propane at the $C_{central}$ via the n-C_3H_7 radical pathway is greater than that at the $C_{terminal}$, whereas the $\delta^{13}C$ value of propane at the $C_{terminal}$ via the i-C_3H_7 radical pathway is greater than that at the $C_{central}$ (Liu et al., 2023). The kinetic isotope effect during kerogen cracking affects the positional isotope composition of propane. Liu et al. (2019) and Zhao et al. (2020) analysed the specific positional carbon and hydrogen isotope compositions of propane in the Arkoma Basin and South Texas shale gas. They found that samples in the high maturity stage ($R_o > 0.6\%$) reached intramolecular equilibrium, whereas those in the maturity stage exhibited non-intramolecular equilibrium characteristics. In this study, the samples from the Upper Paleozoic of the Ordos Basin showed a narrow range of Δ_{C-T} distribution and $R_o < 1.6\%$, indicating that these samples have not reached intramolecular equilibrium, and their isotopic compositions are greatly controlled by kinetic isotope effects.

During kerogen and/or petroleum cracking, k^*/k for reactions involving the loss of radicals increases with temperature (Tang et al., 2000), and the $\delta^{13}C$ value in the precursors become larger (Peterson et al., 2018), resulting in a larger $\delta^{13}C$ value at both terminal and central positions at higher temperatures. The samples in this study also exhibited the same trend.

Kerogen is a complex organic macromolecule with different functional groups and is regarded as a precursor of petroleum and natural gas, which generates hydrocarbons through thermal cracking. During pyrolysis, the carbon atoms in propane produced by C-C bond cleavage undergo primary kinetic isotope effects, whereas the adjacent carbon atoms undergo secondary kinetic isotope effects (Tang et al., 2000; Wang et al., 2024). Kerogen is composed of primary functional groups and isomeric functional groups (such as n-C_3H_7 and i-C_3H_7). During the cracking process, i-C_3H_7, which has lower dissociation energy than n-C_3H_7, preferentially dissociates from kerogen (Hao et al., 2013; Liu et al., 2023).

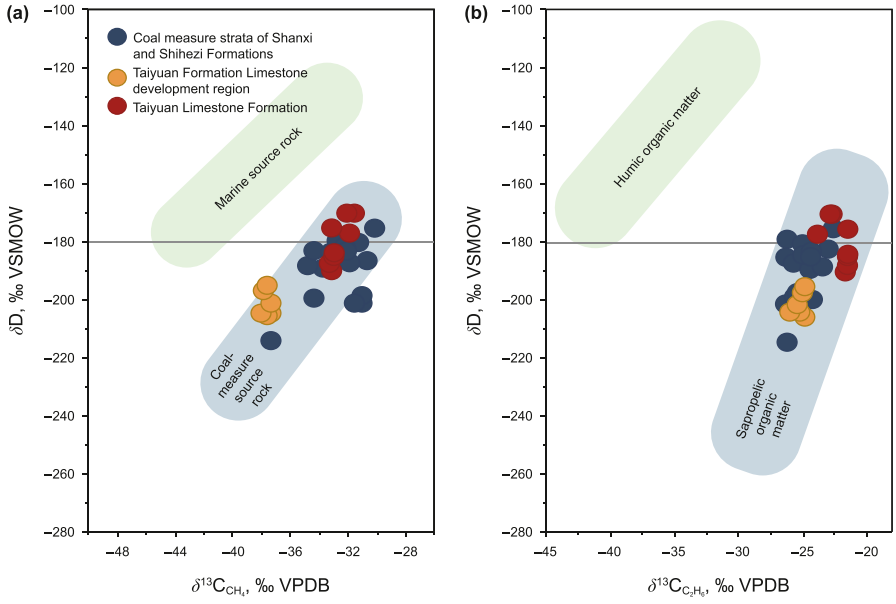

Fig. 10. Hydrogen isotope composition plate of Paleozoic natural gas in the Ordos Basin. **(a)** Scatter plot of $\delta^{13}C_{CH_4}$–δD in natural gas. **(b)** Scatter plot of $\delta^{13}C_{C_2H_6}$–δD in natural gas.

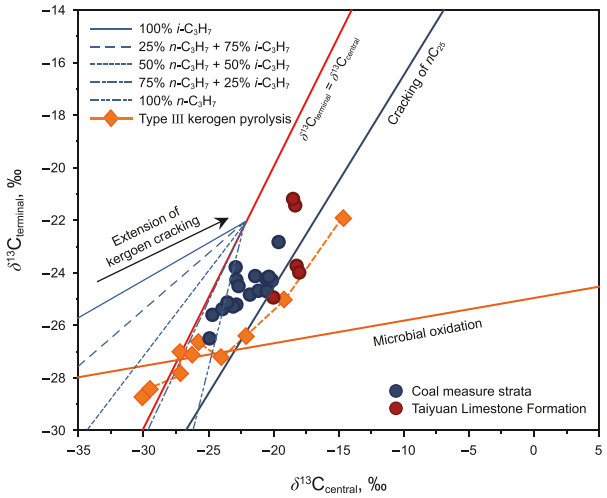

Fig. 11. $\delta^{13}C_{central}$–$\delta^{13}C_{terminal}$ of propane from kerogen cracking based on the rayleigh fractionation model and natural sources. The linear trend illustrating position-specific isotope composition of propane from type III kerogen pyrolysis is after Zhang et al. (2022).

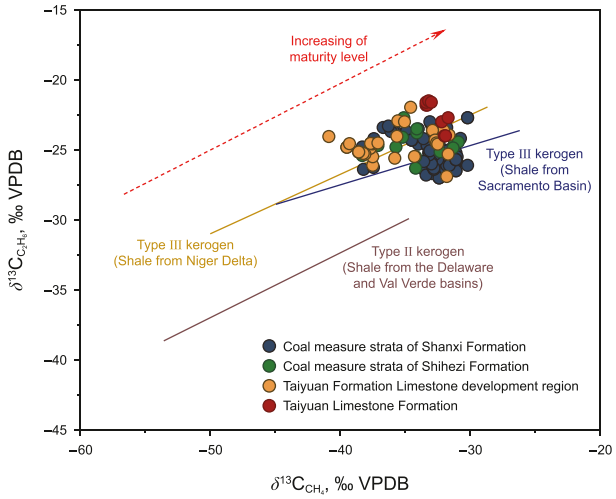

Fig. 13. $\delta^{13}C_{CH_4}$–$\delta^{13}C_{C_2H_6}$ of the hydrocarbon gases originating from different kerogen types. The linear trend of Type II kerogen in shale from the Delaware/Val Verde basins is after Rooney et al. (1995), the linear trend of Type III kerogen in shale from the Sacramento Basin is after Jenden et al. (1988), and the linear trend of Type III kerogen in shale from the Niger Delta is after Rooney et al. (1995).

Therefore, propane is primarily generated through the i-C_3H_7 radical pathway during the low-maturity stage, exhibiting a specific positional carbon isotope composition within the propane molecule, with $\delta^{13}C_{central} < \delta^{13}C_{terminal}$. With increasing maturity and the depletion of isomer groups, the propane generation pathway shifts toward the n-C_3H_7 pathway, leading to a $\delta^{13}C_{central}$ value of propane that is greater than the $\delta^{13}C_{terminal}$ value. The position of propane carbon isotopes changes from $\Delta_{C-T} < 0$ to $\Delta_{C-T} > 0$ as complete intramolecular carbon isotope inversion is achieved, and the R_o maturity increases from 0.46% to 0.50% (Liu et al., 2024). The $\delta^{13}C_1$–R_o formula (Liu and Xu, 1999) was utilized to calculate the R_o value of natural gas in the Taiyuan Limestone Formation, the Taiyuan Formation Limestone development region, the Shanxi Formation and Shihezi Formation, with the minimum R_o value being 0.76%. The reaction pathway has already completed the transformation from i-C_3H_7 to n-C_3H_7, consistent with the measured $\Delta_{C-T} > 0$ results.

Wang et al. (2024) utilized the Rayleigh fractionation model, employing varying ratios of n-C_3H_7 and i-C_3H_7 radicals, to calculate the positional-specific carbon distributions of propane produced from Type III kerogen. The $\delta^{13}C_{central}$–$\delta^{13}C_{terminal}$ value of coal-type gas in the Upper Paleozoic of the Ordos Basin were mainly distributed near the n-C_3H_7 radical trend line (Fig. 11).

Sapropelic organic matter, which originates from plankton and algae, and humic organic matter, which originates from terrestrial plants have different carbon isotopic compositions. The $\delta^{13}C$ value of marine type I kerogen ranged from −30‰ to −28‰ (Buchardt et al., 1986), whereas those of humic organic matter ranged from −27‰ to −22‰ (Whiticar, 1996). The kinetic isotope effects during the thermal degradation of kerogen resulted in the isotopic fractionation of the carbon atoms that participated in bond cleavage (Tang et al., 2000). Thus, the distribution of positional isotopes in propane can be used to identify different types of

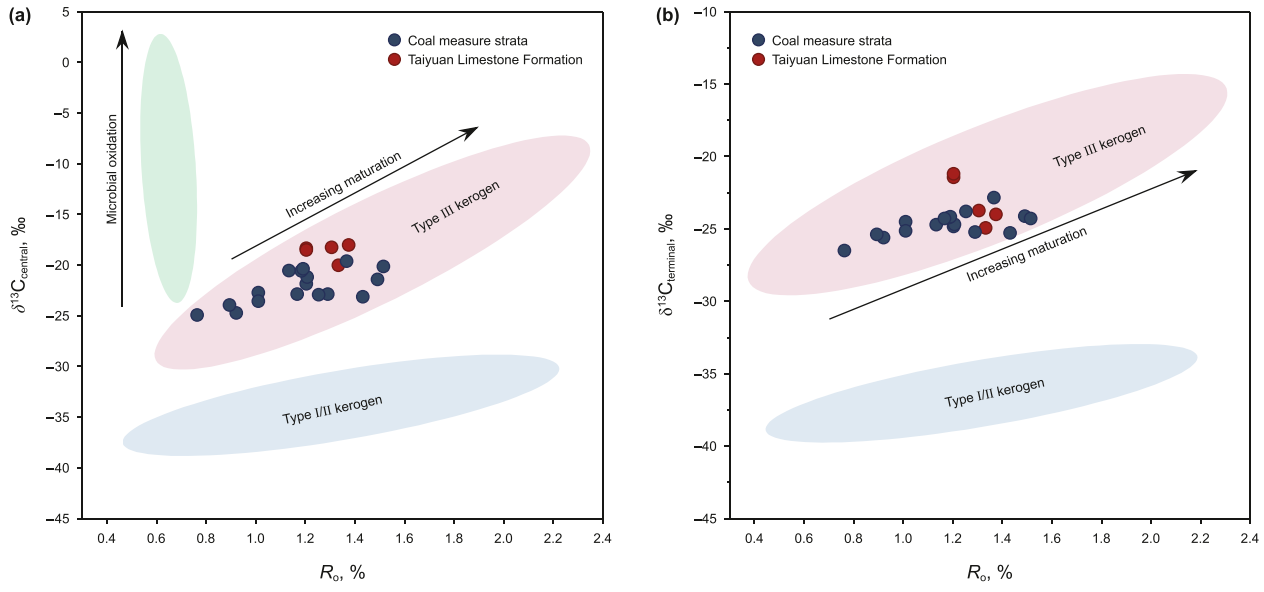

Fig. 12. Relationships of **(a)** $\delta^{13}C_{central}$ and **(b)** $\delta^{13}C_{terminal}$ with the maturity levels of propane in the Paleozoic natural gas, Ordos Basin (modified from Wang et al., 2024).

Table 5
Evaluation standard for marine carbonate source rocks.

Source rock grade	TOC, %	S_1+S_2, mg/g	EOM, %	HC, μg/g
Good	≥ 0.40	≥ 0.30	> 0.03	600–1200
Medium	0.20–0.40	0.10–0.30	0.02–0.03	300–600
Bad	0.10–0.20	0.06–0.10	0.01–0.02	100–300
Not	< 0.10	< 0.06	< 0.01	< 100

precursors (Liu et al., 2023), and helps explain the isotopic anomalies in propane. Wang et al. (2024) utilized the R_o–$\delta^{13}C_{central}$ and R_o–$\delta^{13}C_{terminal}$ relationship plates to determine the type of organic matter in natural gas based on maturity and propane positional isotopic composition. The $\delta^{13}C_{central}$ value of propane generated from type III kerogen pyrolysis are significantly smaller than those from type I/II kerogen. Additionally, the $\delta^{13}C_{central}$ values of propane formed from type I/II and type III kerogens increased with maturation (Fig. 12). The Taiyuan Limestone Formation natural gas and Upper Paleozoic coal measure natural gas also exhibited this correlation characteristic and were clearly classified as Type III kerogen. In the plot correlating $\delta^{13}C_{CH_4}$–$\delta^{13}C_{C_2H_6}$, the distribution trend of Paleozoic natural gas coincided with that of natural gas generated from Type III kerogen in the Niger Delta and Sacramento basins (Fig. 13).

5.3. Geochemical differences of source rocks

The abundance index of organic matter is used to represent the relative content of organic matter in rocks, which is an important index for the evaluation of source rocks (Chen and Liu, 1997). Commonly used evaluation indicators include TOC content and hydrocarbon generation potential (S_1+S_2). Many scholars believe that the process of hydrocarbon generation and expulsion led to a decrease in organic carbon content, so the recovery of organic carbon content should be carried out in carbonate rocks at a high over-maturity stage (Hao, 1984; Qin et al., 2009). Domestic and foreign scholars have studied the evaluation criteria of marine carbonate source rocks. For example, the relationship between hydrocarbon banishment and organic carbon content of carbonate source rocks was studied using simulation experiments, and confirmed that the lower limit of organic carbon in highly-over mature carbonate source rocks was 0.1%–0.25% (Qin et al., 2004); Tengger et al. (2006) used carbon isotopes, rare earth elements, and trace elements to study the carbonate source rocks of the Lower Paleozoic in Ordos and also determined the threshold TOC value as 0.2%. Considering that the loss of organic matter caused by pickling and washing during the experiment may lead to the low content of organic carbon measured in the experiment (Fu, 2023). Hence, the evaluation criteria of marine carbonate source rocks proposed by Han et al. (2018b) were used to evaluate the limestone of Taiyuan Formation (Table 5).

The Permian Taiyuan Limestone Formation in the Ordos Basin had a TOC content of 0.03%–6.11% (average 0.73%) (Table 4), and the S_1+S_2 value of 0.01–2.53 mg/g (average 0.33 mg/g), which can be evaluated as a general-good source rock. However, compared with the Carboniferous–Permian coal and mudstone, the abundance of organic matter is still much lower. R_o of the limestone in the Taiyuan Formation was between 0.6% and 1.4% (the average was 1.1%). Among the 11 samples, the R_o values of 6 samples were approximately 1.4%, and those of 3 samples were approximately 1.0%. The limestone source rocks of the Taiyuan Formation are thus in the late-high maturity stage.

Owing to the high maturity of organic matter in Taiyuan Limestone Formation samples, the rock pyrolysis parameter T_{max} was generally higher than 460 °C, and the type of organic matter by pyrolysis could not be determined using the relationship chart of hydrogen index I_H and T_{max} or oxygen index I_O (Fu, 2023). Therefore, the kerogen composition was identified using polarised light microscopy, and the type of organic matter was identified using the type index TI. The calculation formula was (4). The evaluation criteria was: TI > 80 for type I, 40 ≤ TI ≤ 80 for type II_1, 0 ≤ TI ≤ 40 for type II_2, TI < 0 for type III (Cao, 1985) (Table 6).

$$TI = (\text{sapropelic} \times 100 + \text{exinite} \times 50 - \text{vitrinite} \times 75 - \text{inertinite} \times 100)/100 \quad (4)$$

Because the stable carbon isotopes of kerogen were less affected by maturity, the isotope fractionation effect during thermal evolution also had little effect on the carbon isotope composition. Therefore, the stable carbon isotopes of kerogen were used to classify the types of organic matter. According to SY/T 5737–1995 identification standard, the $\delta^{13}C$ value of hydrocarbon sources in Upper Paleozoic coal rocks and dark mudstones ranged primarily from −27.6‰ to −22.9‰, falling within the typical humic Type III kerogen. The distribution of $\delta^{13}C$ values for the Taiyuan Limestone Formation ranged from −27.8‰ to −24.1‰ (the average value was −25.6‰), slightly lighter. They were classified as type II intermediate–type to type III sapropel–humic kerogen.

Based on the statistical data of the kerogen composition type, the Taiyuan Limestone Formation has favorable kerogen types, primarily composed of algal sapropel and vitrinite groups, with lower contents of liptinites and vitrinite, exhibiting characteristics of Type II–III kerogen, which belongs to the typical mixed input type. There should be the coexistence of aquatic organisms and

Table 6
Statistical table of kerogen components and types of Taiyuan Formation in the Ordos Basin.

Sequence number	Section/well	Exinite, %	Sapropelinite, %	Vitrinite, %	Inertinite, %	TI	Organic matter type	Data source
5	T65	–	67.5	32.0	0.5	43.0	II_1	This study; Fu (2023)
6	Q71	–	50.8	49.2	–	13.9	II_2	
7	Q71	–	44.5	55.0	0.5	2.8	II_2	
12	Y72	–	31.2	68.8	–	−20.4	III	
15	Y93	–	70.0	30.0	–	47.5	II_1	
18	Z4	–	67.4	32.0	0.6	42.8	II_1	
19	M115	–	44.6	54.5	0.9	2.8	II_2	
21	J21	–	68.1	31.0	0.9	43.9	II_1	
24	Y11	–	44.0	55.8	0.2	2.0	II_2	
26	Q2	–	61.5	38.5	–	32.3	II_2	
27	Q71	–	25.4	74.6	–	−40.3	III	
28	M154	–	89.9	10.1	–	82.3	I	
29	Y16	–	66.3	33.7	–	41.0	II_1	
30	ZX6-1	–	68.0	12.0	20.0	39.0	II_2	
31	ZX-10	–	44.0	40.0	16.0	−2.0	III	
32	ZX-15-1	–	86.0	10.0	4.0	74.5	II_1	

terrestrial organisms. During the sedimentary period of the Benxi Formation and Shanxi Formation, the biogenic input of higher plants was obvious, and the $\delta^{13}C$ composition was heavy, regardless of the coal measure source rocks or argillaceous source rocks. It indicates that there was a large source of organic matter of higher plant origin in the Carboniferous–Permian coal measure strata.

In general, the abundance of organic matter in the Taiyuan Limestone Formation was low, and the organic matter was classified as good. The kerogen component was mainly the sapropel group, and the kerogen type was mainly II–III. Most R_o values were higher than 1.2%, indicating late maturity-high maturity evolution stage with a certain hydrocarbon generation potential. Combined with the petrological characteristics, the rock types of Taiyuan Limestone Formation reservoir were mainly algal limestone, bioclastic micrite limestone and bioclastic micrite limestone. The types of reservoir space are rich, mainly dissolution pores, followed by intergranular pores and microcracks. The superimposed combination was developed and the reservoir performance was good (Dong et al., 2023; Fu, 2023; Han et al., 2022). Multiple tectonic movements in the Ordos Basin during the Indochina, Yanshan, and Himalayan movements led to the development of brittle limestone fractures in the Taiyuan Formation, which vertically connected various strata (Xi et al., 2023). Natural gas was aggregated well in limestone reservoirs through faults, cracks, etc. Transport systems.

As the Taiyuan Formation underwent several periods of rapid transgression and slow regression during the depositional period, a sedimentary assemblage of sandstone, limestone, coal stone and mud shale in direct contact was formed in the longitudinal direction. The sand body at the top of the Taiyuan Formation in the study area was not developed, and the limestone was in direct contact with the coal stone and mud shale layers, ensuring good coverage, favorable for natural gas preservation. Meanwhile, the Taiyuan Limestone Formation is situated between the 5# and 8# seams of the Carboniferous–Permian main coal hydrocarbon source rocks (Liu et al., 2023), and directly contacts with multiple thin coal seams (including 8#, 7#, and 6# coal seams) as well as carbonaceous mudstone. The limestone also possesses certain hydrocarbon-generating capacity, collectively forming a typical “sandwich” structural gas reservoir, which endows it with unique natural gas geochemical characteristics. The 8# coal seam is characterized by extensive distribution and considerable thickness (Li Y.N. et al., 2021), effectively sealing the natural gas generated by the underlying coal measure source rocks and preventing large-scale hydrocarbon migration from the Lower Paleozoic oil-type gas into the Taiyuan Limestone Formation reservoir. Additionally, the thick gypsum-salt layer in the Ordovician Majiagou Formation of the Lower Paleozoic exhibits excellent sealing capacity, further isolating the Lower Paleozoic oil-type gas from the Taiyuan Limestone Formation gas reservoir.

6. Conclusions

In recent years, two horizontal wells deployed in the Lower Permian Taiyuan Limestone Formation reservoir in the central–eastern Ordos Basin have made breakthroughs. Gas testing yielded high flow rates, with daily production exceeding one million cubic meters, indicating that the Taiyuan Limestone Formation reservoir has good potential for resource development. Analysing the geochemical characteristics of natural gas in limestone reservoirs and comparing the carbon and hydrogen isotopic compositions of gas with those of Upper Palaeozoic sandstone gas are crucial for clarifying the genesis of limestone-derived natural gas.

The $\delta^{13}C_{CH4}$ values of natural gas in the Upper Paleozoic Taiyuan Limestone Formation in the Ordos Basin ranged from −33.4‰ to −31.7‰, whereas $\delta^{13}C_{C_2H_6}$ ranged between −24.0‰ and −21.5‰. The positive correlation between contents and carbon isotope of methane and ethane showed homology. Distinguished from the ‘self-generated and self-accumulated’ oil-type gas in the Paleozoic sub-salt strata, it was consistent with the typical coal-type gas characteristics of the Upper Paleozoic.

The Δ_{C-T} values of Taiyuan Formation natural gas samples were all greater than 0, ranged from 2.6‰ to 5.9‰. The minimum R_o value, calculated through $\delta^{13}C_{CH_4}$, was 0.76%, indicating that propane was predominantly formed via the n-C_3H_7 radical pathway. Utilized the R_o–$\delta^{13}C_{central}$ and R_o–$\delta^{13}C_{terminal}$ relationships, the gas was identified to be originated from type III humic kerogen.

The limestone of the Taiyuan Formation was evaluated as general-good source rock, and the organic matter type was good. The kerogen composition was dominated by sapropel and vitrinite, mainly of types II–III. The source material for hydrocarbon formation was a mixture of lower aquatic organisms and terrigenous organisms. R_o values were mostly above 1.2%, indicating a mature to highly mature evolutionary stage with certain hydrocarbon generation potential. However, the hydrocarbon generation potential is substantially lower than that of the Carboniferous–Permian coal measure source rocks, and its contribution to the Taiyuan Limestone Formation gas reservoir is limited. It still depends on the natural gas accumulation of adjacent coal measure source rocks.

CRediT authorship contribution statement

Wen Zhang: Writing – review & editing, Writing – original draft, Investigation, Data curation. **Qian-Ping Wang:** Resources. **Wen-Hui Liu:** Writing – review & editing, Supervision, Funding acquisition. **Ping-Ping Shi:** Resources. **Hou-Yong Luo:** Writing – review & editing, Funding acquisition. **Peng Liu:** Writing – review & editing. **Xiao-Yan Chen:** Supervision. **Qian Zhang:** Writing – review & editing. **Xiao-Feng Wang:** Supervision. **Dong-Dong Zhang:** Supervision. **Yi-Ran Wang:** Investigation. **Fu-Qi Li:** Investigation.

Declaration of competing interests

The authors declare that they have no known competing financial interests or personal relationships that could have appeared to influence the work reported in this paper.

Acknowledgements

This research was financially sponsored by the National Natural Science Foundation of China (Grant Nos. 41930426, 42172173, 42230815) and the PetroChina Changqing Oilfield Innovation Consortium Project (Grant No. 2024D1JC06).

References

Buchardt, B., Clausen, J., Thomsen, E., 1986. Carbon isotope composition of lower Palaeozoic kerogen: effects of maturation. Org. Geochem. 10 (1), 127–134. https://doi.org/10.1016/0146-6380(86)90016-1.

Cao, Q.Y., 1985. Identification of microcomponents and types of kerogen under transmitted light. Petrol. Explor. Dev. 5, 14, 23+81–88. https://doi.org/CNKI:SUN:SKYK.0.1985-05-002 (in Chinese).

Chen, Q.H., Li, K.Y., Zhang, D.F., et al., 2010. The relationship between fan delta and hydrocarbon accumulation in Benxi Taiyuan Formation, Ordos Basin. Geology in China 37 (2), 421–429. https://doi.org/10.3969/j.issn.1000-3657.2010.02.015 (in Chinese).

Chen, S.Y., Liu, H.J., 1997. Carboniferous-permian lithofacies and paleogeography in the eastern part of the north China platform. Regional Geology of China (4) 44–51. https://doi.org/CNKI:SUN:DZXE.0.2008-10-001 (in Chinese).

Dai, J.X., 1992. Identification of various types of alkane gas. Science China (B: Chemistry, Life Sciences, Geology) (2), 185–193. https://doi.org/10.1360/yb1992-35-10-1246 (in Chinese).
Dai, J.X., 2011. Significance of the study on carbon isotopes of alkane gases. Nat. Gas. Ind. 31 (12), 1–6+123. https://doi.org/10.3787/j.issn.1000-0976.2011.12.001 (in Chinese).
Dai, J.X., Li, J., Luo, X., et al., 2005. Stable carbon isotope compositions and source rock geochemistry of the giant gas accumulations in the Ordos Basin, China. Org. Geochem. 36 (12), 1617–1635. https://doi.org/10.1016/j.orggeochem.2005.08.017.
Dai, J.X., Zou, C.N., Liao, S.M., et al., 2014. Geochemistry of the extremely high thermal maturity Longmaxi shale gas, southern Sichuan Basin. Org. Geochem. 74, 3–12. https://doi.org/10.1016/j.orggeochem.2014.01.018.
Dai, J.X., Zou, C.N., Zhang, S.C., et al., 2008. Identification of alkane gas of inorganic origin and organic origin. Science China (D: Earth Sci.) 38 (11), 1329–1341. https://doi.org/CNKI:SUN:JDXK.0.2008-11-001 (in Chinese).
Dong, G.D., Liu, X.S., Pei, W.C., et al., 2023. Characteristics and main controlling factors of tight limestone reservoir in Taiyuan Formation of Ordos Basin. Nat. Gas Geosci. 34 (6), 1018–1027. https://doi.org/10.11764/j.issn.1672-1926.2023.02.005 (in Chinese).
Fu, J.H., 2023. Accumulation characteristics and exploration potential of tight limestone gas in the Taiyuan Formation of the Ordos Basin. Earth Sci. Front. 30 (1), 20–29. https://doi.org/10.13745/j.esf.sf.2022.8.24 (in Chinese).
Fu, J.H., Li, S.X., Niu, X.B., et al., 2020. Geological characteristics and exploration of shale oil in Chang 7 Member of Triassic Yanchang Formation, Ordos Basin, NW China. Petrol. Explor. Dev. 47 (5), 931–945. https://doi.org/10.1016/S1876-3804(20)60107-0.
Fu, J.H., Liu, X.S., Wei, L.B., et al., 2022. Breakthrough and significance of natural gas exploration in the fourth member of Majiagou Formation of subsalt Ordovician in Ordos Basin. China Petroleum Exploration 27 (2), 47–58. https://doi.org/10.3969/j.issn.1672-7703.2022.02.005 (in Chinese).
Fu, S.T., Tian, J.C., Chen, H.D., et al., 2003. The Delta depositional system distribution of late Paleozoic Era in ordos Basin. J. Chengdu Univ. Technol. (Sci. Technol. Ed.) 30 (3), 236–241. https://doi.org/CNKI:SUN:CDLG.0.2003-03-001 (in Chinese).
Fu, Y.H., 2023. Evaluation of Hydrocarbon Generation Potential of Taiyuan Formation Limestone in Central and Eastern Ordos Basin. School of Geosciences Yangtze University (in Chinese).
Gilbert, A., Yamada, K., Suda, K., et al., 2016. Measurement of position-specific ^{13}C isotopic composition of propane at the nanomole level. Geochem. Cosmochim. Acta 177, 205–216. https://doi.org/10.1016/j.gca.2016.01.017.
Guo, X.S., Zhou, D.H., Zhao, P.R., et al., 2022. Progresses and directions of unconventional natural gas exploration and development in the Carboniferous-Permian coal measure strata, Ordos Basin. Oil Gas Geol. 43 (5), 1013–1023. https://doi.org/10.11743/ogg20220501 (in Chinese).
Han, W.X., Luo, X., Tao, S.Z., et al., 2022. Effect of in-situ hydrocarbon generation over geochemical properties of the reservoired natural gas: A case study from the Ordos Basin, China. J. Petrol. Sci. Eng. 214, 110575. https://doi.org/10.1016/j.petrol.2022.110575.
Han, W.X., Ma, W.J., Tao, S.Z., et al., 2018a. Carbon isotope reversal and its relationship with natural gas origins in the Jingbian gas field, Ordos Basin, China. Int. J. Coal Geol. 196, 260–273. https://doi.org/10.1016/j.coal.2018.06.024.
Han, W.X., Ma, W.J., Tao, S.Z., et al., 2018b. Hydrocarbon generation potential evaluation of upper Paleozoic limestone in Ordos Basin. Earth Sci. 43 (2), 599–609. https://doi.org/10.3799/dqkx.2017.529 (in Chinese).
Hao, Y.L., Zhang, H., Li, J., 2013. Molecular simulation on pyrolysis mechanism of butane. Acta Pet. Sin. 29, 824–829. https://doi.org/10.3969/j.issn.1001-8719.2013.05.013.
Hao, S.S., 1984. Richness of organic matter and its evolutional characteristics in carbonate source rocks. Exp. Pet. Geol. 6 (1), 67–71. https://doi.org/10.11781/sysydz198401067 (in Chinese).
Hu, A.P., Li, J., Zhang, W.Z., et al., 2007. Comparison of geochemical characteristics and genetic types of natural gas in Upper Paleozoic, Lower Paleozoic and Mesozoic in Ordos Basin. Science China (D: Earth Sci.) 37 (S2), 157–166. https://doi.org/10.1360/zd2007-37-zkII-157 (in Chinese).
Huang, S.P., Fang, X., Liu, D., et al., 2015. Natural gas genesis and sources in the Zizhou gas field, Ordos Basin, China. Int. J. Coal Geol. 152, 132–143. https://doi.org/10.1016/j.coal.2015.10.005.
Jenden, P.D., Kaplan, I.R., Poreda, R., et al., 1988. Origin of nitrogen-rich natural gases in the California Great Valley: Evidence from helium, carbon and nitrogen isotope ratios. Geochem. Cosmochim. Acta 52 (4), 851–861. https://doi.org/10.1016/0016-7037(88)90356-0.
Jin, B., Rolle, M., 2016. Position-specific isotope modeling of organic micropollutants transformation through different reaction pathways. Environ. Pollut. 210, 94–103. https://doi.org/10.1016/j.envpol.2015.11.014.
Julien, M., Nun, P., Hohener, P., et al., 2016. Enhanced forensic discrimination of pollutants by position-specific isotope analysis using isotope ratio monitoring by ^{13}C nuclear magnetic resonance spectrometry. Talanta 147, 383–389. https://doi.org/10.1016/j.talanta.2015.10.010.
Kong, Q.F., Yao, J.L., Ren, J.F., et al., 2024. Sources and exploration potential of Ordovician subsalt natural gas in Ordos Basin. Nat. Gas Geosci. 35 (7), 1187–1201. https://doi.org/10.11764/j.issn.1672-1926.2023.12.009 (in Chinese).
Li, C., Zhang, D.F., Zheng, X.P., et al., 2024. Genesis and distribution patterns of limestone reservoirs of the Lower Permian Taiyuan Formation in Hengshan gas field, Ordos Basin. Marine Origin Petroleum Geology 29 (3), 257–268. https://doi.org/10.3969/j.issn.1672-9854.2024.03.004 (in Chinese).
Li, F.R., Liu, W.H., Wang, X.F., et al., 2023. Geochemical characteristics and genesis of Paleozoic natural gas in the Ordos Basin. Petroleum Geology & Experiment 45 (4), 809–820. https://doi.org/10.11781/sysydz202304809 (in Chinese).
Li, J., Li, J., Li, Z.S., et al., 2014. The hydrogen isotopic characteristics of the Upper Paleozoic natural gas in Ordos Basin. Org. Geochem. 74, 66–75. https://doi.org/10.1016/j.orggeochem.2014.01.020.
Li, J., Li, J., Li, Z.S., et al., 2018. Characteristics and genetic types of the Lower Paleozoic natural gas, Ordos Basin. Mar. Petrol. Geol. 89, 106–119. https://doi.org/10.1016/j.marpetgeo.2017.06.046.
Li, J., Zhang, C.L., Jiang, F.J., et al., 2021. The hydrogen isotopic characteristics of the Upper Paleozoic natural gas in Ordos Basin. Org. Geochem. 41 (4), 30–40. https://doi.org/10.1016/j.orggeochem.2014.01.020 (in Chinese).
Li, L.L., 2018. Hydrocarbon generation and expulsion history of source rocks and natural gas accumulation period in the Upper Paleozoic of the Linxing Block, Ordos Basin. China University of Petroleum, Beijing (in Chinese).
Li, Y.N., Liu, W.H., Wang, X.F., et al., 2021. Potential causes of depleted $\delta^{13}Ccarb$ excursions in Ordovician marine carbonates, Ordos Basin, China. Mar. Petrol. Geol. 134, 105331. https://doi.org/10.1016/j.marpetgeo.2021.105331.
Liu, C.J., Liu, P., McGovern, G.P., et al., 2019a. Molecular and intramolecular isotope geochemistry of natural gases from the Woodford Shale, Arkoma Basin, Oklahoma. Geochem. Cosmochim. Acta 255, 188–204. https://doi.org/10.1016/j.gca.2019.04.020.
Liu, P., Wang, X.F., Liu, C.J., et al., 2023a. Kinetic isotope effect and reaction pathways of thermogenic propane generation at early maturation stage: Insights from position-specific carbon isotope distribution. Mar. Petrol. Geol. 153, 106252. https://doi.org/10.1016/j.marpetgeo.2023.106252.
Liu, P., Wang, X.F., Liu, C.J., et al., 2024. Intramolecular carbon isotopic rollover in propane from natural gas reservoirs of the Shantanu Basin: Insights into chemical structure of kerogen. Org. Geochem. 188, 104740. https://doi.org/10.1016/j.orggeochem.2024.104740.
Liu, Q.Y., Chen, M.J., Liu, W.H., et al., 2009. Origin of natural gas from the Ordovician paleo-weathering crust and gas-filling model in Jingbian gas field, Ordos Basin, China. J. Asian Earth Sci. 35 (1), 74–88. https://doi.org/10.1016/j.jseaes.2009.01.005.
Liu, Q.Y., Dai, J.X., Li, J., et al., 2008. Hydrogen isotope composition of natural gases from the Tarim Basin and its indication of depositional environments of the source rocks. Sci. China Earth Sci. 51 (2), 300–311. https://doi.org/10.1007/s11430-008-0006-7.
Liu, Q.Y., Jin, Z.J., Meng, Q.Q., et al., 2015. Genetic types of natural gas and filling patterns in Daniudi gas field, Ordos Basin, China. J. Asian Earth Sci. 107, 1–11. https://doi.org/10.1016/j.jseaes.2015.04.001.
Liu, Q.Y., Wu, X.Q., Wang, X.F., et al., 2019b. Carbon and hydrogen isotopes of methane, ethane, and propane: A review of genetic identification of natural gas. Earth Sci. Rev. 190, 247–272. https://doi.org/10.1016/j.earscirev.2018.11.017.
Liu, W.H., Wang, X.F., Zhang, D.D., et al., 2022. Restudy on geochemical characteristics and genesis of Jing Bian gas field in Ordos Basin. J. NW Univ. 52 (6), 943–956. https://doi.org/10.16152/j.cnki.xdxbzr.2022-06-004 (in Chinese).
Liu, W.H., Xu, Y.C., 1999. A two-stage model of carbon isotopic fractionation in coal-gas. Geochimica 28 (4), 359–366. https://doi.org/10.19700/j.0379-1726.1999.04.006 (in Chinese).
Liu, X.S., Huang, D.J., Hu, J.L., et al., 2024. Reservoir characteristics of Carboniferous Benxi Formation coal-rock gas in the central and eastern Ordos Basin. Nat. Gas. Ind. 44 (10), 51–62. https://doi.org/CNKI:SUN:TRQG.0.2024-10-003 (in Chinese).
Liu, X.S., Zhang, T., Huang, D.J., et al., 2023b. New breakthrough in and direction of natural gas exploration in Taiyuan Formation limestone in the central and eastern Ordos Basin. Nat. Gas. Ind. 43 (5), 1–11. doi: CNKI:SUN:TRQG.0.2023-05-001. (in Chinese).
Luo, S.S., Fu, Y.H., Yin, J., et al., 2024. Lithofacies types and geochemical characteristics of carbonate source rocks in Taiyuan Formation of middle and eastern Ordos Basin. Journal of Yangtze University (Natural Science Edition) 21 (1), 19–31. https://doi.org/10.16772/j.cnki.1673-1409.20230307.001 (in Chinese).
Mao, Y.H., 2020. Study on Sedimentary Characteristics and Lithofacies Palaeogeography of Early Permian Taiyuan Formation in the Eastern Ordos Basin. China University of Geosciences, Beijing (in Chinese).
Ma, Y.S., Mei, M.X., Chen, X.B., et al., 1999. Sedimentology of Carbonate reservoirs. Geological Publishing House, Beijing.
Milkov, A.V., 2021. New approaches to distinguish shale-sourced and coal-sourced gases in petroleum systems. Org. Geochem. 158, 104271. https://doi.org/10.1016/j.orggeochem.2021.104271.
Ni, Y.Y., Zhang, J.C., Yao, L.M., et al., 2024. Application of carbon and hydrogen isotopes in the natural gas origin study. Nat. Gas Geosci. 35 (11), 1897–1909. https://doi.org/10.11764/j.issn.1672-1926.2024.05.007 (in Chinese).
Peterson, B.K., Formolo, M.J., Lawson, M., 2018. Molecular and detailed isotopic structures of petroleum: kinetic Monte Carlo analysis of alkane cracking. Geochem. Cosmochim. Acta 243, 169–185. https://doi.org/10.1016/j.gca.2018.09.012.
Qin, J.Z., Liu, B.Q., Guo, J.Y., et al., 2004. Discussion on the evaluation standards of Carbonate source rocks. Petroleum Geology & Experiment 26 (3), 281–286. https://doi.org/10.11781/sysydz200403281 (in Chinese).
Qin, J.Z., Tengger, Fu, X.D., 2009. Study of forming condition on marine excellent source rocks and its evaluation. Petroleum Geology & Experiment 31 (4), 366–372+378. https://doi.org/10.11781/sysydz200904366 (in Chinese).
Rooney, M.A., Claypool, G.E., Moses Chung, H., 1995. Modeling thermogenic gas generation using carbon isotope ratios of natural gas hydrocarbons. Chem. Geol. 126 (3), 219–232. https://doi.org/10.1016/0009-2541(95)00119-0.
Tang, Y., Perry, J.K., Jenden, P.D., et al., 2000. Mathematical modeling of stable carbon isotope ratios in natural gases. Geochem. Cosmochim. Acta 64 (15), 2673–2687. https://doi.org/10.1016/S0016-7037(00)00377-X.
Tengger, Liu, W.H., Xu, Y.C., et al., 2006. Comprehensive geochemical identification of highly evolved marine carbonate source rocks - a case study of Ordos Basin.

Science China (D: Earth Sci.) 36 (2), 167–176. https://doi.org/CNKI:SUN:JDXK.0.2006-02-005 (in Chinese).
Wang, K.L., Zhong, S.K., Zhao, W.B., et al., 2024. Impact of diagenetic one volution of reservoirs of Taiyuan Formation limestone in Ordos Basin. J. Chengdu Univ. Technol. (Sci. Technol. Ed.) 51 (5), 772–786. https://doi.org/10.3969/j.issn.1671-9727.2024.05.05 (in Chinese).
Wang, X.F., Liu, P., Liu, W.H., et al., 2024. Intramolecular carbon isotope of propane from coal-derived gas reservoirs of sedimentary basins: Implications for source, generation and post-generation of hydrocarbons. Geosci. Front. 15 (4), 101806. https://doi.org/10.1016/j.gsf.2024.101806.
Wang, X.F., Liu, W.H., Shi, B.G., et al., 2015. Hydrogen isotope characteristics of thermogenic methane in Chinese sedimentary basins. Org. Geochem. 83 (84), 178–189. https://doi.org/10.1016/j.orggeochem.2015.03.010.
Wang, T., Wang, X.F., Zhang, D.D., et al., 2025. Pore formation and evolution mechanisms during hydrocarbon generation in organic-rich marl. Pet. Sci. 22 (2), 557–573. https://doi.org/10.1016/j.petsci.2024.10.011.
Whiticar, M.J., 1996. Stable isotope geochemistry of coals, humic kerogens and related natural gases. Int. J. Coal Geol. 32 (1), 191–215. https://doi.org/10.1016/S0166-5162(96)00042-0.
Wu, X.Q., Ni, C.H., Chen, Y.B., et al., 2019. Source of the Upper Paleozoic natural gas in the Dingbei area, Ordos Basin, China. Journal of Natural Gas Geoscience 4 (4), 183–190. https://doi.org/10.1016/j.jnggs.2019.08.001.
Xi, S.L., Li, M.R., Zhao, W.B., et al., 2023. Accumulation conditions, key exploration and development technologies of large-scale Hengshan gas field in Ordos Basin. Acta Pet. Sin. 44 (6), 1015–1028. https://doi.org/CNKI:SUN:SYXB.0.2023-06-010 (in Chinese).
Xiao, D., Tan, X.C., Zhang, D.F., et al., 2019. Discovery of syngenetic and eogenetic karsts in the Middle Ordovician gypsum-bearing dolomites of the eastern Ordos Basin (Central China) and their heterogeneous impact on reservoir quality. Mar. Petrol. Geol. 99, 190–207. https://doi.org/10.1016/j.marpetgeo.2018.10.004.
Xiao, W.H., Lei, F.P., Ma, G.F., et al., 2024. The main controlling factors for natural gas enrichment in the Taiyuan Formation in the Yanchi area of the western Ordos Basin. Nat. Gas Geosci. 36 (4), 580–591. https://doi.org/10.11764/j.issn.1672-1926.2024.09.003 (in Chinese).
Xiong, Y., Tan, X.C., Dong, G.D., et al., 2020. Diagenetic differentiation in the Ordovician Majiagou Formation, Ordos Basin, China: Facies, geochemical and reservoir heterogeneity constraints. J. Petrol. Sci. Eng. 191, 107179. https://doi.org/10.1016/j.petrol.2020.107179.
Yang, H., Bao, H.P., Ma, Z.R., 2014. Reservoir-forming by lateral supply of hydrocarbon: A new understanding of the formation of Ordovician gas reservoirs under gypsolyte in the Ordos Basin. Nat. Gas. Ind. 34 (4), 19–26. https://doi.org/10.3787/j.issn.1000-0976.2014.04.003 (in Chinese).
Yang, H., Liu, X.S., Yan, X.X., et al., 2015. Discovery and reservoir-forming geological characteristics of the Shenmu Gas Field in the Ordos Basin. Nat. Gas. Ind. B 2 (4), 295–306. https://doi.org/10.1016/j.ngib.2015.09.002.
Yang, S.R., 2022. Biogenic composition and organic matter enrichment mechanism of shallow water platform source rocks: A case study from the Ordovician pre-salt Carbonate rocks in Ordos Basin. China University of Petroleum, Beijing (in Chinese).
Yang, X.L., Gao, J., He, F.W., et al., 2025. Sedimentary evolution and reservoir-forming conditions of Taiyuan Formation in Jiaxian area, eastern margin of Ordos Basin. Nat. Gas Geosci. 36 (1), 86–96. https://doi.org/10.11764/j.issn.1672-1926.2024.08.001 (in Chinese).
Yao, J.L., Hu, X.Y., Fan, L.Y., et al., 2018. The geological conditions, resource potential and exploration direction of natural gas in Ordos Basin. Nat. Gas Geosci. 29 (10), 1465–1474. https://doi.org/10.11764/j.issn.1672-1926.2018.08.008 (in Chinese).
Yu, J., Ma, T., Miao, C.H., et al., 2015. Analysis of components in refinery gas by Agilent 7890A gas chromatograph. Contemp. Chem. Ind. 44 (5), 1179–1181+1184. https://doi.org/10.13840/j.cnki.cn21-1457/tq.2015.05.102 (in Chinese).
Zhang, J., 2012. Evaluation of Upper Paleozoic Source Rocks in Eastern Ordos Basin. Xi'an Shiyou University (in Chinese).
Zhang, L., Li, Y., Jiang, W.M., et al., 2022. Position-specific carbon isotopic composition of thermogenic propane: Insights from pyrolysis experiments. Org. Geochem. 166, 104379. https://doi.org/10.1016/j.orggeochem.2022.104379.
Zhang, Q., Liu, W.H., Zhang, W., et al., 2024. Carbon isotope geochemistry and its geological significance in the Jixian system of the Qishan section, Ordos Basin. Palaeogeogr. Palaeoclimatol. Palaeoecol. 650, 112347. https://doi.org/10.1016/j.palaeo.2024.112347.
Zhang, T., Gong, X.K., Huang, Z., et al., 2024. Micro characteristics and formation mechanism of low-quality gas reservoirs in Taiyuan Formation of Shenmu Gas Field, Ordos Basin. Petroleum Geology & Experiment 46 (1), 32–45. https://doi.org/10.11781/sysydz202401032 (in Chinese).
Zhang, W., Liu, W.H., Wang, X.F., et al., 2023. Geochemical characteristics of natural gas in Upper Middle and Lower Paleozoic assemblages in the Middle East, Ordos Basin. Nat. Gas Geosci. 34 (10), 1842–1854. https://doi.org/10.11764/j.issn.1672-1926.2023.05.002.
Zhao, D.F., 2013. Study on the Accumulation Characteristics of Tight Sandstone Gas Reservoirs in the Upper Paleozoic of the Eastern Ordos Basin. Xi'an Shiyou University (in Chinese).
Zhao, H., Liu, C.J., Larson, T.E., et al., 2020. Bulk and position-specific isotope geochemistry of natural gases from the Late Cretaceous Eagle Ford Shale, South Texas. Mar. Petrol. Geol. 122, 104659. doi: 12210.1016/j.marpetgeo.2020.104659.
Zhao, J.Z., Zhang, W.Z., Li, J., et al., 2014. Genesis of tight sand gas in the Ordos Basin, China. Org. Geochem. 74, 76–84. https://doi.org/10.1016/j.orggeochem.2014.03.006.